3D BIOPRINTED CARDIAC PATCHES FOR CARDIOVASCULAR REGENERATIVE MEDICINE

A Thesis
Presented To
The Academic Faculty

by

Gabriella Kabboul

In Partial Fulfillment
of the Requirements for the Degree
Bachelor of Science in the
Wallace H. Coulter Department of Biomedical Engineering

Georgia Institute of Technology
May 2021

3D BIOPRINTED CARDIAC PATCHES FOR CARDIOVASCULAR REGENERATIVE MEDICINE

Approved by:

Dr. Vahid Serpooshan
Department of Biomedical Engineering
Georgia Institute of Technology

Dr. David H. Frakes
Department of Biomedical Engineering
Georgia Institute of Technology

Date Approved: 6 May 2021

To my parents, Fadi and Marie Claire, and my sister, Nicole.

ACKNOWLEDGEMENTS

I would like to thank Dr. Vahid Serpooshan for allowing me to take part in this research and for all his support throughout. I would also like to thank the Serpooshan Lab, particularly, Bo Hwang for their guidance and mentorship.

TABLE OF CONTENTS

LIST OF TABLES

LIST OF FIGURES

ABSTRACT

Myocardial infarction (MI) is the leading cause of death worldwide causing irreversible damage to the heart. Despite the incidence and prevalence of MI, current treatments delay the progression of the damage rather than regenerate the function of the cardiac tissue. Over the past years, there has been a rising interest in cardiac tissue engineering, and three-dimensional (3D) bioprinting, to design regenerative approaches to treat damage to the heart caused by MI. Particularly, bioengineered cardiac patches have shown their potential in restoring cardiac tissue structure and function. Regardless of this progress, the clinical application of current cardiac tissue engineering platforms remains limited by shortcomings, ranging from poor vascularization to reduced cellular survival. This study investigated the fabrication of perfusable 3D bioprinted cardiac patches with functional vascular networks. Cardiac patch devices were 3D bioprinted with gelatin methacrylate (gelMA) hydrogel with channels bioprinted using a sacrificial pluronic bioink. The cardiac constructs were seeded with human umbilical vein endothelial cells (HUVECs) and cultured in static, dynamic, and perfusion conditions throughout a two-week period to evaluate *in vitro* the cellular growth and organization within the channels. The results from this study suggested that the 3D model of the patch was successfully bioprinted with the formation of fully patent and endothelialized channels. Although no significant differences were found in cellular metabolic activity between static and dynamic conditions at all timepoints, perfused cardiac patches showed a decrease in cellular metabolic activity at day 10 and day 14. Furthermore, qualitative results indicated the successful attachment of HUVECs on the channel walls. Overall, these results suggest that the developed cardiac patch devices serve as a potential model to repair and restore *in vitro* cardiac tissue after MI. In addition, novel 3D bioprinted vascularized cardiac

constructs can be used as research enabling an *in vitro* platform to provide insights into cardiac tissue homeostasis, diseases, and therapies.

CHAPTER 1

INTRODUCTION

Heart failure (HF) due to myocardial infarction (MI) is the leading cause of morbidity and mortality worldwide affecting over 700,000 people per year [1-3]. MI can be attributed to multiple causes, such as mechanical valve complications, comorbidities as hypertension, malignant arrythmias, among others, which cause a local hypoxia in the myocardium. Eventually, continued ischemia in the myocardium causes the loss of cardiomyocytes. However, the limited capability for post-natal proliferation of cardiomyocytes as terminally differentiated cells results in diminished cardiac function, dilatation of the cardiac chambers, and thinning of the chamber walls following the ischemic injury [4, 5]. Ultimately, these processes lead to overall irreversible cardiac dysfunction, terminating in HF.

Currently, heart transplantation remains the main treatment for end-stage HF [6]. Nonetheless, heart transplants remain highly invasive as the transplanted heart can be rejected by cellular and antibody mediated responses. Most impactfully, heart transplantations are restricted by the reduced number of heart donors [1]. Although other treatments, such as ventricular assist devices, cellular cardiomyoplasties, and immunotherapies have been implemented to repair cardiac tissue post-MI, their main objective is to palliate symptoms and delay the progression of HF rather than counteract the loss of functional tissue [4, 7]. Despite promising results, cardiac engineering continues to advance to target therapeutics for tissue repair after irreversible damage to the heart.

In recent years, tissue engineering and, in particular, three-dimensional (3D) bioprinting have evolved as alternative means to design tissue constructs, used as cardiac patches, with remarkable

regenerative properties. Engineering cardiac patch devices that can repair heart tissue has been of great interest as a potential therapy in promoting cardiomyocyte regeneration and restoring cardiac functions [8]. Predominantly, 3D bioprinting has emerged as a technique to generate scaffold systems by controlling the geometry of constructs while designing customizable and reproducible structures for tissue regeneration applications [9, 10]. However, recent advances in tissue engineered patch devices remain limited by the insufficiency in their biocompatibility, functional vascularization, reproducibility, and cell survival and functionality characteristics.

To address these issues, this work aims to develop and evaluate *in vitro* an engineered vascularized patch model for cardiac tissue regeneration addressing the challenges in MI treatments to date. We investigate the fabrication of 3D bioprinted cardiac patch devices with perfusable vasculature, which can promote regeneration of damaged myocardium after MI. To this end, the cardiac constructs are bioprinted with gelatin methacrylate (gelMA) hydrogel, while a sacrificial pluronic bioink is used to print an interconnected vascular channel network within the 3D construct. To evaluate the function of the bioprinted patches, the constructs are endothelialized with human umbilical vein endothelial cells (HUVECs) and subjected to cell culturing throughout a two-week time period in static, dynamic (rocking), or perfusion culture conditions.

We hypothesize that the geometry and biomaterials of the 3D bioprinted cardiac patch systems, consisting of gelMA hydrogel and sacrificial pluronic bioink, support the attachment, growth, and metabolism of HUVECs and, therefore, can be used to create endothelialized perfusable microvessels in the bioprinted devices. In addition, as gelMA has been gaining increasing attention over the past decade for its biological cues and shape integrity, we hypothesize

that the use of gelMA in bioprinting contributes to the formation of biocompatible cardiac patch systems with high structural fidelity and survival of HUVECs within the pre-engineered channels [11, 12]. Furthermore, the printability of sacrificial pluronic as a bioink has motivated its use in 3D bioprinting. Once degraded at low temperatures, we hypothesize that the printed pluronic allows the formation of microchannels intrinsic to the bioprinted cardiac patches. With respect to the culture conditions, a significant difference in cellular growth among static, dynamic, and perfusion is hypothesized. Particularly, an increase in HUVEC metabolic activity is predicted for the perfused cardiac constructs.

Here, we demonstrated that the 3D model was successfully bioprinted with gelMA hydrogel and pluronic bioink with the formation of fully patent channels. Furthermore, results showed that the seeded HUVECs had significant attachment, proliferation, and formed a smooth, uniform, and relatively mature endothelium in the vascular networks. However, no significant differences in cellular metabolic activity and proliferation were observed between the static and dynamic culture throughout the 14-day period suggesting that these conditions do not provide a significant difference in optimal environments for cell growth and endothelialization. However, the perfused cardiac patches showed a significant decrease in cellular metabolic activity beginning at day 7 compared to static and rocking groups. These could be attributed to possible HUVEC detachment and loss as a result of built-up wall shear stress in the perfused channels, suggesting that further optimization would be required to design more robust *in vitro* perfusion systems. In general, we evaluated *in vitro* the geometry and culture conditions required to design 3D bioprinted patches for cardiac tissue regeneration providing an alternative strategy to engineer patch devices that are

highly reproducible, biocompatible, and with functional endothelialization of the pre-formed vasculature to repair cardiac tissue after MI.

CHAPTER 2

LITERATURE REVIEW

In recent years, there has been a heightened emphasis towards developing regenerative technologies that can repair ischemic cardiac tissue due to MI, particularly as it is the leading cause of death owing to cardiovascular diseases [1, 2]. As cardiomyocytes have low self-renewing properties, following MI, their limited ability to regenerate leads to irreversible cardiovascular diseases and, eventually, to HF. The most successful treatment for end-stage HF to date is heart transplantation, which is a highly invasive procedure limited by the stagnation in heart donors' supply and high immune risks of rejection [1, 6]. Thus, throughout the last decade, myriad tissue engineering platforms have developed as alternatives to fabricate systems aimed to repair damaged cardiac tissue. Despite progress, the fabrication and clinical application of cardiac constructs that are reproducible, biocompatible, and with functional vasculature remains to be established. Therefore, there is a clear need for novel techniques to design and fabricate cardiac device systems to repair and recover damage to the myocardium and address challenges in current MI treatments.

Among a variety of strategies to engineer cardiac patches for regenerative medicine, 3D bioprinting has gained increasing attention as an innovative manufacturing technique presenting a wide assortment of advantages [10, 13]. 3D bioprinting allows precise spatial control of biomaterials, cells, and biological factors to fabricate functional constructs while manipulating the geometry, the integration of nano and microstructures, and direct cellular organization. By these means, bioprinting has the potential of designing 3D functional patch devices with biomimetic properties resembling those of the native cardiac microenvironment and ECM [14, 15]. Given the rising significance of 3D bioprinting for cardiac regeneration, research has focused on

investigating a variety of 3D bioprinting approaches: extrusion-based and inkjet-based. The most commonly used method is extrusion-based bioprinting, which has been implemented for layer-by-layer deposition of inks through a syringe-like assembly at constant flows, pressures, and printing speeds and is best used for bioinks of low or high viscosities; nevertheless, it is limited by the low printing fidelity and resolution [14, 16, 17]. Particularly, Kolesky et al. printed cardiac constructs through extrusion under applied pressurized air [16]. However, the authors noted that the desired printed filament was dependent upon the alterations in the printing speeds, pressure, nozzle diameter, and height from the printing plate. In another study, Hinton et al. suggested that extrusion-based bioprinting is preferred when printing with soft materials subject to losing their 3D structure and when attempting to control the volume being extruded [18]. In contrast, inkjet-based bioprinting has been used for deposition of inks as droplets. It is preferred solely for bioinks with low viscosities and has been shown to have less printing resolution compared to extrusion-based bioprinting [6, 14, 19]. Moreover, a review by Kyle et al. highlighted the disadvantages of inkjet bioprinting focusing on the small volume of droplets in dimensions of pico-liters minimizing the ability to print larger, real-size structures [17]. Regardless of the bioprinting method, the biomaterials enabling printability and biological cues of patch systems have yet to be specified.

While there is an extensive body of literature precising the selection of biomaterials for tissue regeneration, the biocompatibility and fidelity of the biomaterials to mimic the native cardiac ECM and microenvironment remain a clinical challenge [20]. Hydrogels are preferred given their polymeric, hydrophilic chains and their ability to simulate the biochemical and physical properties of the cardiac ECM [21]. Naturally-derived hydrogels, such as collagen or gelatin, are biocompatible and biodegradable, but lack the mechanical strength to support the surrounding

tissue [21]. Contrarily, synthetically-derived hydrogels, such as poly(ethylene glycol), have high mechanical stiffnesses, but present deficiencies in their biocompatibility to the inborn tissue [21]. Thus, a blend of natural and synthetic hydrogels would be effective to design cardiac patches with regenerative applications [22]. Specifically, the use of gelMA, a hydrogel based on collagen and cross-linked methacrylate side groups, has been gaining increasing interest for its hybrid properties. Particularly, Bejleri et al. claimed that gelMA is effective for regenerative medicine purposes as it has enhanced biomimetic properties and biological cues with the surrounding tissue [20]. Furthermore, Yue et al. suggested the facile tunability and effective polymerization using UV light as a photo-initiator to provide ideal structure and stiffness for the patch [23]. However, the effects of the selected biomaterials on cardiac patch geometry remain unresolved.

Despite progress in the development of 3D bioprinted cardiac patches, one of the most significant limitations is construct geometry hindering the diffusion of oxygen and nutrients, which enforces restrictions on the construct thickness, biomaterials, and cellular growth. Without oxygen and nutrients, cells would not have means of survival and the patch functionality would be impacted. In particular, according to Radisic et al., the inclusion of pre-engineered vasculature in 3D bioprinted patches simulate the capillaries of the body and expand the thickness of clinically relevant cardiac patches to ranges between 1 to 5 mm [24]. Therefore, vascularization represents a pre-requisite for tissue regeneration. To this end, in recent years, researchers have been incorporating vascular networks embedded within the patches using fugitive materials, such as sacrificial pluronic bioink that is removed through dilution at low temperatures, leaving hollow microvessels for cells to form as a layer of endothelium [25]. Kolesky et al. suggested the fabrication of constructs with vascular networks ramifying into branches simulating the capillaries

[26]. In their study, the patch was printed with gelMA and the vasculature with pluronic bioink. Conversely, the printed vasculature was prone to swelling given the diffusion of water within the patch, suggesting that a different geometry and diameter of the embedded networks are required, such that it mimics the vasculature in the body ranging from larger to smaller channels and such that there is sufficient space between vessels to tolerate any diffusion of water. Withal, dependent on the successful oxygen and nutrient diffusion within cardiac constructs is the selection of cells to proliferate and remain metabolically active.

Currently, there is conflicting research on the most effective cells that could be used for 3D bioprinting of cardiac patch constructs. Multiple cell types can be added to cell-laden bioinks, or instead, cell-free bioinks could be utilized. Previous research has shown that HUVECs seeded in constructs with endothelial growth medium endothelialize the vascular networks enabling oxygen and nutrient diffusion as well as functional metabolic activity of the patch [22, 25-28]. Other studies have implemented cells such as mesenchymal stem cells [29], epicardial mesothelial cells [30], or induced pluripotent stem cells (iPSCs) [6], which can differentiate and proliferate into cardiomyocytes and mimic the native cardiac tissue more effectively. Regardless of the cells chosen, studies have demonstrated that cellular proliferation and metabolic activity is augmented under conditions, such as rocking or perfusion, which is a result of enhanced cell-to-cell communication [26]. However, further studies are required to conclude the effects of culture conditions on cell growth and proliferation.

Previous studies have attempted to design and test cardiac patches for myocardium regeneration after MI but have been limited by a wide assortment of shortcomings, ranging from

limited oxygen and nutrient diffusion to low cellular survival due to the lacking signaling of biological cues necessary to promote cell growth and proliferation. Therefore, the aim of this study is to investigate the fabrication of perfusable cardiac patch systems with pre-engineered vasculature and evaluate *in vitro* the function of the patch devices through the formation of smooth and mature endothelium of the intrinsic vascular network as a potential novel cardiac patch system that overcomes current challenges for improved recovery of cardiac function post-MI. Here, the cardiac patch is 3D bioprinted with gelMA hydrogel for the construct and sacrificial pluronic bioink for the embedded channel network. Overall, the fabrication of 3D bioprinted patches with incorporation of vascular networks is reported and the perfusion of cardiac patches and formation of hollow microvessels (microcapillaries) is assessed. This study addresses the endothelialization of the vasculature in static, dynamic, and perfused culture conditions as well as monitors cellular metabolic activity, attachment, and proliferation. Further, the patch geometry and culture conditions required for endothelialization of these constructs are studied to determine the efficacy of this platform to design constructs that can potentially have regenerative medicine properties to better recover cardiac function after MI.

CHAPTER 3

METHODOLOGY

The design and fabrication of perfusable 3D bioprinted cardiac patches for cardiac tissue regeneration is a result of manipulating the biomaterials to mimic the cardiac microenvironment as well as the 3D bioprinting technique to design the precise geometry with vascular networks of the cardiac patch devices. Here, cell survival, growth, and the formation of endothelium were analyzed by measuring cellular metabolic activity and through qualitative imaging with immunostaining to gauge cellular organization and morphology within the channels of the patches.

Bioink Preparation

To 3D bioprint the cardiac constructs, gelMA bioink at 10% (w/v) was synthesized from porcine gelatin type A and methacrylic anhydride as described in previous reports [31, 32]. The concentration of the gelMA bioink was chosen based on the high printability and stability of the bioink filament during the bioprinting extrusion as well as the high cell viability of gelMA at this concentration [33]. To print the intrinsic network of vascular channels, a sacrificial pluronic bioink at 38% (w/v) was prepared by dissolving pluronic with phosphate-buffered saline (PBS). As a thermosensitive material, pluronic bioink was synthesized at this concentration to exhibit controlled printability and shear-thinning of the printed filaments [34].

Design of Cardiac Patch Structures

The 3D model of the cardiac patch with perfusable vascular channels was created as a computer-aided design (CAD) model using Autodesk Fusion360® software (Autodesk, Inc., USA). The cardiac patch geometry featured a disk structure with dimensions of 15 mm in diameter and 3

mm in thickness (**Figure 1**). The modeled vascular network intrinsic to the disk-shaped construct followed a 1-2-4-2-1 ramification structure beginning at a microvessel diameter of 1.4 mm, which bifurcated in two channels of 1 mm in diameter, and then ramified once again in two branches of 0.7 mm in diameter to mimic the ramification of vessels and capillaries within the cardiac system. The patch has a single inlet and a single outlet to provide an interface between the scaffold and the perfusion system. After designing the construct, the CAD model of the cardiac patches was converted to the standard stereolithography (STL) format file for printing.

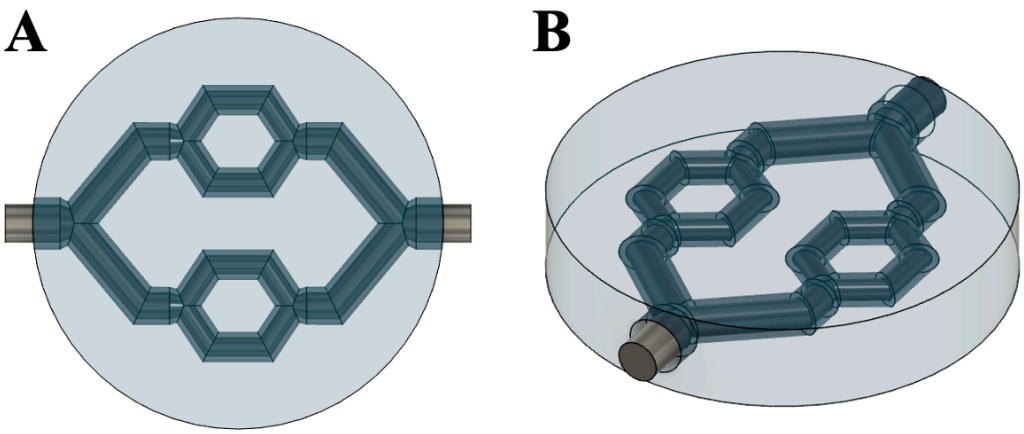

Figure 1. Design of the Cardiac Patch Device. 3D design of the disc-shaped cardiac patch with pre-engineered vascular networks. Top perspective of the cardiac patch (**A**). Lateral perspective of the cardiac patch (**B**). The cardiac construct is 15 mm in diameter and 3 mm in thickness. Following a 1-2-4-2-1 structure, the network of vascular channels within the disc-shaped construct has a diameter of 1.4 mm, 1 mm, and 0.7 mm, respectively, with a single inlet and outlet.

3D Bioprinting of Cardiac Patches

A multi-extruder 3D bioprinter with three printheads (BioX, CELLINK) was implemented to 3D bioprint the constructs. The cardiac patches were printed using 10% (w/v) gelMA mixed with 0.5% (w/v) Irgacure photoinitiator, which allows absorbance of the UV light for photo-crosslinking. The microvessels were printed with 38% (w/v) sacrificial pluronic bioink, which

degrades at low temperatures. A temperature-controlled pneumatic extrusion-based printhead was employed to print with gelMA because of its thermo-reversible properties. A standard pneumatic extrusion-based printhead was used to print with pluronic with respective printing parameters (**Table 1**). Subsequently, the bioprinted constructs were crosslinked with UV light at 2.5 mW/cm^2 for 45 seconds on each side of the patch to ensure adequate and uniform mechanical stiffness to promote cell growth. The cardiac patches were then incubated in PBS at 4°C for 4 hours for the pluronic to degrade and generate hollow microvessels within the gelMA patch.

Table 1. Printing Parameters for BioX, CELLINK 3D Bioprinter.

Parameter	**Dimensions for GelMA Printing**	**Dimensions for Pluronic Printing**
Nozzle Gauge	27 gauge	27 gauge
Temperature	23°C	22.5°C
Speed	6 mm/s	4 mm/s
Pressure	35 kPa	80 kPa

Cell Culture of Printed Cardiac Patches

Cell seeding of the printed patches was performed manually *in vitro* to assess the cellular growth and metabolic activity of the cultured cells, with the goal of creating a uniform and continuous endothelium covering onto the channels. Prior to cell seeding, the luminal surface of the channels was coated with fibrin hydrogel. For this purpose, the fibrin coating was done with fibrinogen treatment at 1 mg/ml for 2 hours followed by thrombin enzyme at 2 U/ml for 30 minutes at 37°C. Subsequently, we prepared 60 µl of solution consisting of HUVECs suspended in the endothelial growth media (VEGF LS-1020) at a density of 16 million cells/ml. Cell suspension was injected through the inlet of the printed construct into the fibrin-coated channels and incubated at 37°C for 7 days in static condition to promote cell attachment and growth. After the 7-day

culture in static, the cellular constructs were introduced to one of the following culture conditions: static, dynamic (rocking), and perfusion.

Perfusion of Printed Cardiac Patches

The bioprinted cardiac patches were inserted into a custom designed 3D printed chamber, which was connected to a peristaltic pump bioreactor system for perfusion to evaluate the formation of fully patent channels and test the perfusion culture conditions on the viability and growth of HUVECs in the microchannels (**Figure 2**). A 3D printed chamber was used to house the cardiac patch. Tubing with an inner diameter of 1.52 mm served to connect the bioprinted housing to a reservoir of HUVEC media. The bioreactor system was maintained in an incubator at 37°C to ensure adequate temperature for cellular growth. During a one-week perfusion culture period, endothelial growth media was flown through the HUVEC-seeded vascular channels at a flow rate of 111 µl/min to simulate the blood flow in small vessels.

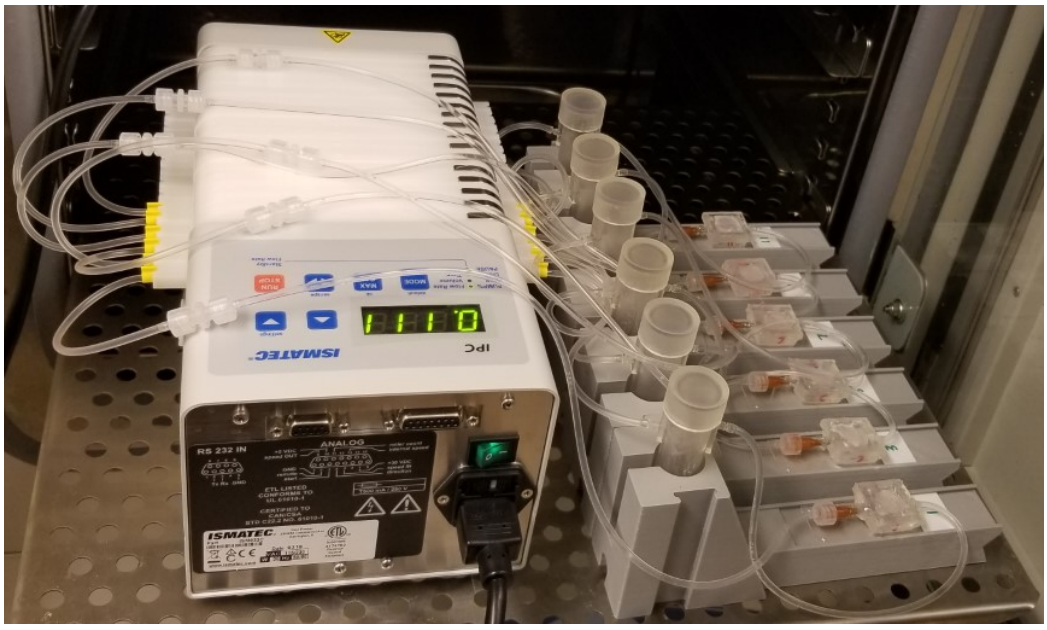

Figure 2. Bioreactor Perfusion Pump Setup. A setup of the perfusion bioreactor system implemented to pump HUVEC media through the vascular channels embedded within the cardiac patches. The cardiac constructs were inserted into customized 3D printed chambers, shown to the right. The peristaltic pump

bioreactor, shown to the left, was connected to the 3D printed chambers, which housed the 3D bioprinted cardiac patches, through tubing with an inner diameter of 1.52 mm. The HUVEC media was flown through the HUVEC-seeded vascular networks at a flow rate of 111 µl/min.

Analyzing Cell Viability and Proliferation

The cardiac constructs were tested with a noninvasive AlamarBlue assay throughout a two-week culture period. The percentage of AlamarBlue reduction was used to quantitatively analyze the changes in cellular metabolic activity levels, as a measure of cell viability and growth [35, 36]. Constructs were incubated with the AlamarBlue assay (AlamarBlue® Cell Viability Reagent, BioRad) at 37°C for 4 hours in static culture conditions. The cardiac constructs in dynamic (rocking) culture conditions were maintained on a rocker at 60 revolutions/min for the 4 hours of AlamarBlue incubation time. For the perfused patches, 10% AlamarBlue solution was added to the media reservoir and was run for 4 hours. To measure the percentage of reduced reagents, the media was sampled from each construct after 4 hours and the absorbance of the solution was measured at wavelengths of 550 nm and 660 nm via a microplate reader (BioTek™ Synergy™ 2 Multi-Mode Microplate Reader). This viability and metabolic activity assay was performed at days 3, 7, 10, and 14 during the *in vitro* culture.

Immunohistochemistry and Confocal Microscopy

At days 7 and 14 of the culture period, the cardiac patches were fixed in 4% paraformaldehyde and stained to assess cell morphology and organization within the vascular channels. Constructs were stained against 4′,6-diamidino-2-phenylindole (DAPI) as a cell nucleus marker, wheat germ agglutinin (WGA) to stain cell membrane, and CD31 as an endothelial cell marker to gauge the organization and morphology of cells. The stained constructs were then imaged using a confocal laser scanning microscope (Olympus FV1000) to qualitatively assess the formation of endothelium

in the pre-engineered vasculature and the organization and morphology of HUVECs in the channel walls.

Statistical Analysis

All results presented are expressed as mean ± standard error of the mean (SEM). A one-way ANOVA was used to determine statistically significant differences in AlamarBlue reduction, which positively correlates to cellular metabolic activity, within the culture conditions of cardiac patches at day 3, 7, 10, and 14, respectively. Consecutively, a post-hoc Tukey-Kramer was performed for multiple comparisons between culture conditions. Particularly, a p-value < 0.05 was considered statistically significant (* p-value < 0.05, ** p-value < 0.01, **** p-value < 0.0001).

CHAPTER 4

RESULTS

3D Bioprinted Cardiac Patches

The CAD model of the cardiac patches was successfully 3D bioprinted with 10% (w/v) gelMA hydrogel and the channel network was effectively bioprinted with 38% (w/v) sacrificial pluronic bioink (**Figure 3**). Furthermore, perfusing the microvessels with endothelial growth media demonstrated that the pluronic bioink successfully degraded at 4°C and thereby generated fully patent channels within the hydrogel constructs.

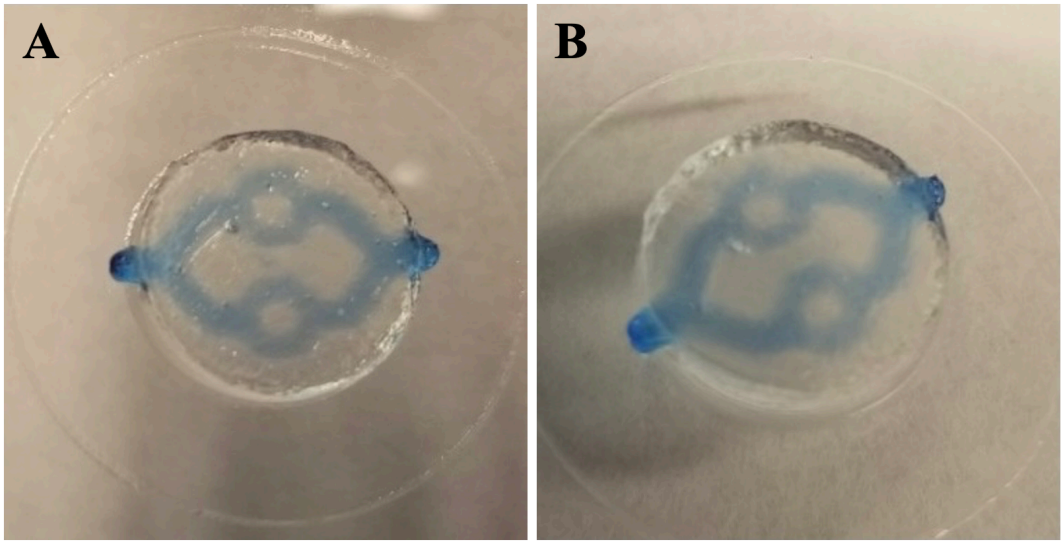

Figure 3. Bioprinted Cardiac Patches. The CAD model of the cardiac patch system successfully 3D bioprinted using gelMA with vascular networks printed utilizing pluronic. Top perspective of the cardiac patch (**A**). Lateral perspective of the cardiac patch (**B**).

Endothelial Cell Viability and Growth in Cardiac Patches

To assess the biocompatibility of the bioinks used for the development of the cardiac patches and to assess the HUVEC culture conditions, the percentage of AlamarBlue reduction was determined at days 3, 7, 10, and 14 of static, dynamic (rocking), and perfusion culture conditions

(**Figure 4**). AlamarBlue results indicated that HUVECs remained viable and metabolically active throughout the 14-day culture in static, rocking, and perfusion conditions. In addition, day 7 resulted in statistically the greatest levels of AlamarBlue reduction across all timepoints. Particularly, in rocking and perfusion, the AlamarBlue reduction was measured at 20.83 $\pm$ 0.99 % and 22.85 $\pm$ 0.24 %, respectively. In contrast, in static culture conditions, the changes in cellular metabolic activity were greatest for day 14 (22.83 $\pm$ 1.37 %) with a non-significant difference compared to day 7 (22.61 $\pm$ 1.52 %).

Statistically significant differences in AlamarBlue reduction were determined among culture conditions within 3D bioprinted cardiac patches at days 3, 7, 10, and 14, respectively. At day 3 and day 7, no significant differences were found in AlamarBlue reduction for patches in static, rocking, or perfusion conditions. At day 10 and day 14, there was no significant difference in AlamarBlue reduction between static and rocking conditions. However, there was a statistically significant decrease (p-value < 0.0001) in cell viability between cardiac patches in static and perfusion culture conditions as well as in rocking and perfusion conditions at days 10 and 14.

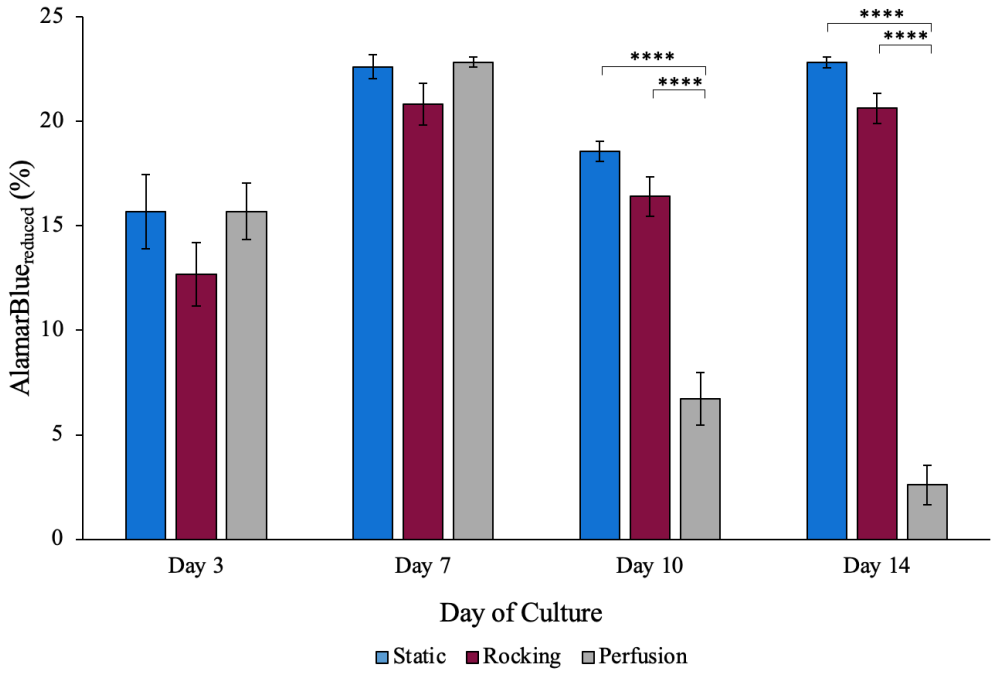

Figure 4. Characterization of Endothelial Cell Viability and Growth in 3D Bioprinted Cardiac Patches. Cellular metabolic activity of HUVECs seeding in the vascular networks of the 3D bioprinted cardiac patches measured by the percentage of AlamarBlue reduction throughout a 14-day *in vitro* culture in static, dynamic (rocking), and perfusion conditions (n = 4 per group). Results reported as mean ± SEM. * p-value < 0.05, ** p-value < 0.01, **** p-value < 0.0001.

Endothelialization of the Vascular Channels

The organization and morphology of HUVECs cultured within the vasculature was assessed by confocal microscopy. As alamarBlue assay results showed greatest cell viability and growth for cardiac patches in the static culture, in comparison to constructs in rocking or perfusion, immunofluorescence imaging was performed on static cardiac constructs. Furthermore, as day 7 showed the greatest cellular metabolic activity consistent among all conditions, the confocal imaging was performed on constructs at day 7. For the cardiac patches stained against DAPI, WGA, and CD31, confocal microscopy imaging of the channels at bifurcations 1, 2, and 4 indicated effective attachment and proliferation of HUVECs within the walls of the vascular networks (**Figure 5**). GFP staining demonstrated viable HUVECs lined up on the channel walls of

the cardiac patch (**Figure 6**). In addition, HUVEC nuclei staining (DAPI) demonstrated the formation of layers of endothelium on the lumen area of the vasculature; however, the coverage of HUVECs was not uniform within the walls of the channels (**Figure 7**). This could be attributed, at least partly, to the gravitational forces exerted onto the seeded HUVECs, which highlights the need for future studies to improve cellularization of printed constructs (e.g., flipping the constructs post seeding to achieve a more uniform cell distribution).

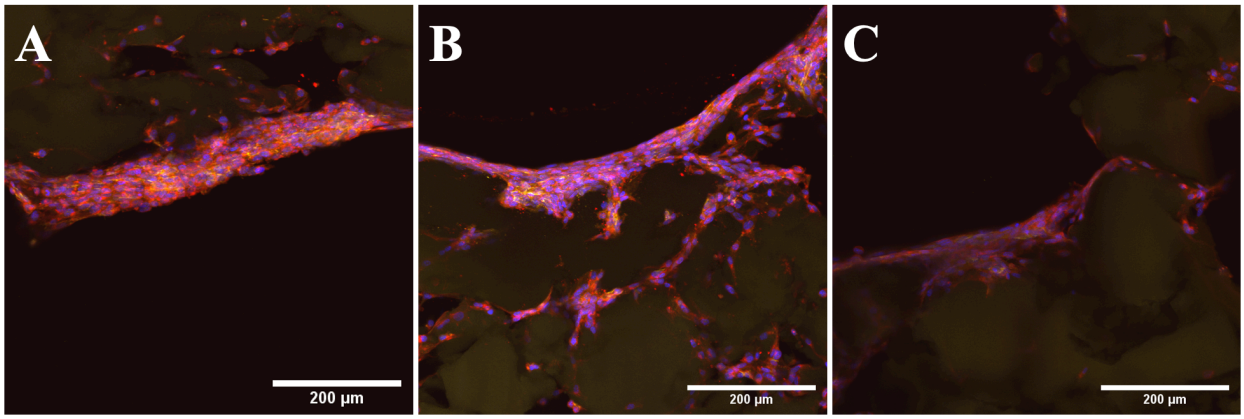

Figure 5. Characterization of HUVEC Organization and Morphology in the Microchannels of the 3D Bioprinted Cardiac Patches. Cardiac patches with perfusable vascular networks seeded with HUVECs were stained against DAPI (blue), WGA (red), and CD31 (green). The channels of the cardiac patches organized in a 1-2-4-2-1 structure were visualized through confocal microscopy. Immunofluorescence imaging of channel bifurcation 1 (**A**), 2 (**B**), 4 (**C**) in static culture conditions at day 7. Scale bars: 200 µm.

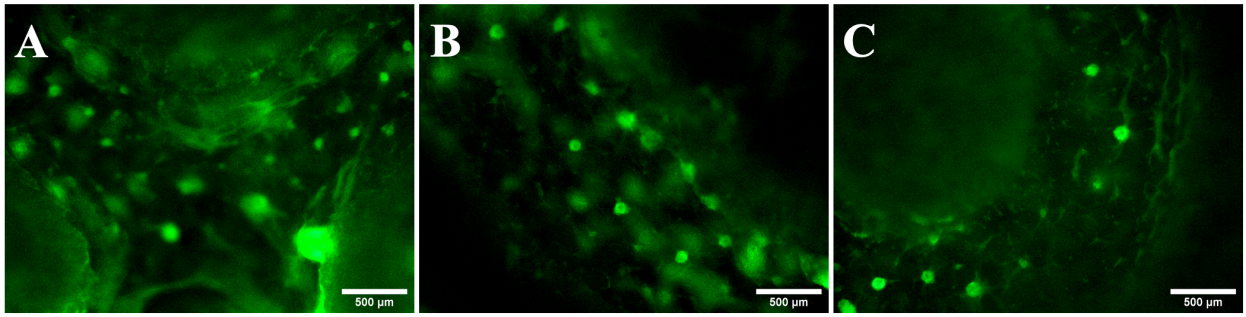

Figure 6. HUVEC Attachment in the Microchannels of the 3D Bioprinted Cardiac Patches. Representative GFP (green) images of live HUVECs attached to the walls of the microchannels at bifurcation 1 (**A**), 2 (**B**), 4 (**C**) of the bioprinted cardiac constructs in static conditions at day 7. Scale bars: 500 µm.

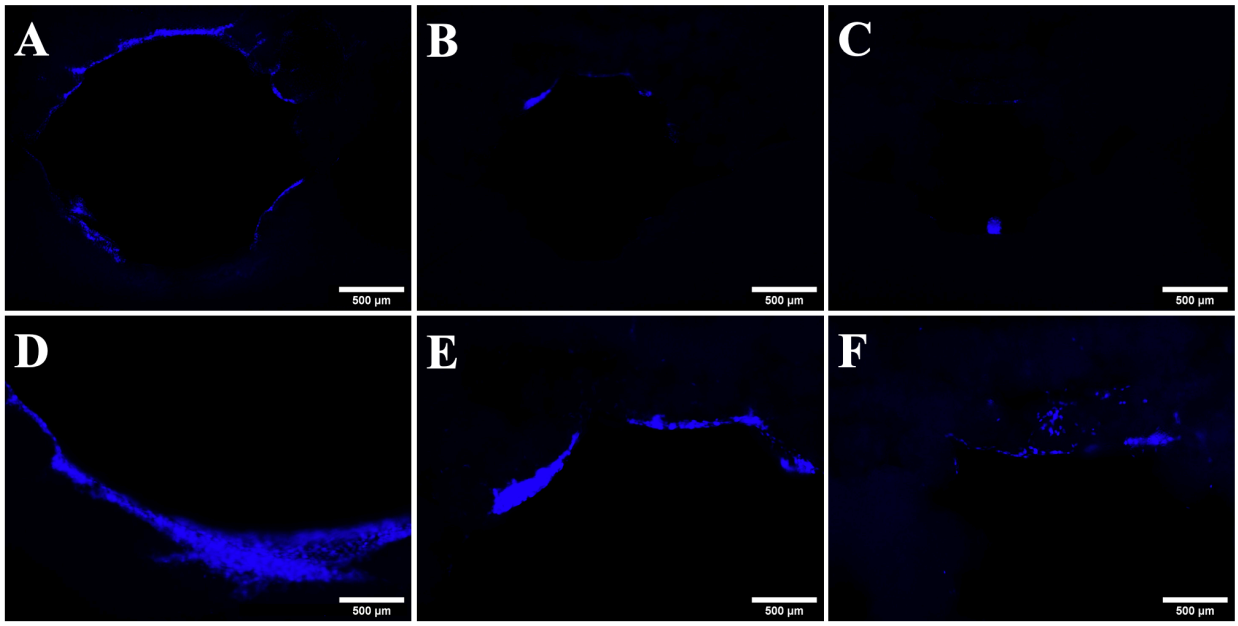

Figure 7. Coverage of HUVECs in the Microchannels of the 3D Bioprinted Cardiac Patches. Immunofluorescence imaging staining against DAPI (blue) to gauge the coverage of HUVEC nuclei within the lumen area of the vascular networks to characterize the endothelialization of the microchannels of the cardiac patches in static conditions at day 7. Imaging of channel bifurcations 1 (**A**, **D**), 2 (**B**, **E**), and 4 (**C**, **F**) at 4x (**A**, **B**, **C**) and 10x (**D**, **E**, **F**) magnification. Scale bars: 500 µm.

CHAPTER 5

DISCUSSION

Bioengineered cardiac patch devices have been developed over the past years and have shown to be effective in regenerating cardiac tissue after MI. Particularly, cardiac constructs made of ECM with seeded cells have suggested to be effective in repairing cardiac tissue and promoting cardiomyocytes after an ischemic injury. Nonetheless, the utilization and translation of these scaffolds to clinical settings have been limited due to the lack of biological cues to promote tissue regeneration, poor vascularization, and consequently, reduced cell survival and functionality. To overcome these shortcomings, we investigated the fabrication of a 3D bioprinted cardiac patch system with perfusable vasculature and applied this platform *in vitro* to study the viability and growth of HUVECs within the microchannels of the patches. Our results demonstrate high-fidelity bioprinting of the cardiac patches utilizing gelMA bioink. Intrinsic microchannel networks, printed with sacrificial pluronic bioink, established stable and perfusable vascular mimics. The 3D design supported the attachment and metabolic activity of HUVECs seeded within the channels and exhibited *in vitro* a functional vasculature with mature endothelium. Thereby, these results indicate that the cardiac patch design is an effective vehicle for cell survival and proliferation, which overall leads to a better 3D model to repair and regenerate *in vitro* cardiac tissue after MI.

Design and Material Characterization of Bioprinted Cardiac Patches

In comparison to other strategies to generate 3D scaffolds, such as hydrogel molding (casting), electrospinning, and 3D spheroid systems, bioprinting offers unique advantages in fabricating organized 3D patches with precise architectural and spatial control of the geometry [10, 13]. Therefore, over the past years, there has been a rising interest in 3D bioprinting as it has been

reported to generate anatomically and physiologically complex constructs mimicking native tissue while accurately printing with multiple materials and cells [16]. However, despite progress in 3D bioprinting for cardiac regenerative medicine, the designs of the constructs thus far have shown to have limited bioactivity and restricted oxygen and nutrient diffusion resulting in scaffolds that do not support functional activities of cardiomyocytes nor promote cardiac tissue regeneration. Consequently, this study utilized 3D bioprinting to address current challenges in cardiac patch designs. Here, clinically thick disk-shaped constructs were successfully printed using gelMA with pre-engineered vascular networks following a 1-2-4-2-1 structure printed with pluronic using a multi-extruder bioprinter (**Figure 3**). The embedded vasculature was precisely printed which allowed the designed cardiac patch channels to be comparable to small arteries or arterioles. The geometry control offered by extrusion-based bioprinting at controlled nozzle gauge, printing speeds, temperature, pressure, and nozzle-plate distance showed effective printing of the cardiac patch device (**Table 1**).

However, crucial to the fabrication of 3D bioprinted cardiac scaffolds with intrinsic vasculature is the design of cardiac patches that are biocompatible and photo-crosslinkable with facile tunability and high printing fidelity. Therefore, gelMA hydrogel was used to print the cardiac patch devices as it has been shown to have superior tunable physicochemical characteristics and biocompatibility. Nevertheless, despite the great potential of gelMA as a hydrogel, the concentration of gelMA that offers high printing fidelity and mechanical stiffness while sustaining biological cues and promoting cellular survival remains a challenge. Prior studies have shown that gelMA at concentrations greater than 15% (w/v) have strong shape fidelity but low cellular survival [37] while gelMA at less than 5% (w/v) has shown high cell viability but low structural

printability [38]. Thus, printing with gelMA at 10% (w/v) could allow high-fidelity printing with high cell bioactivity. Likewise, 38% (w/v) pluronic bioink, a fugitive thermosensitive material which degrades at low temperatures, was used to print the vascular networks of the patch devices. The sacrificial pluronic once degraded at 4°C could generate hollow microchannels in the patch. Effectively, from this study, the optimal shape fidelity of the gelMA and pluronic bioinks after bioprinting the cardiac patch systems demonstrated that they could be used to print in 3D disk-shaped constructs and complex small vessels similar in size to capillaries. Particularly, after perfusion of the vascular networks at a physiological flow rate, we demonstrated that the cardiac patch maintained the integrity of fully patent channels, which once again demonstrates the adequate printability and mechanical properties of gelMA and pluronic to design perfusable 3D cardiac constructs.

Evaluation of Cellular Growth and Viability *In Vitro* in Bioprinted Cardiac Patches

To assess effectiveness of the designed 3D structure of the cardiac patch and the selection of biomaterials, the function of printed patches with perfusable vasculature was evaluated *in vitro* in static, dynamic (rocking), and perfusion culture conditions. The channels of the constructs were seeded with HUVECs and cultured throughout a two-week period to form smooth and mature endothelium. AlamarBlue assay was run at days 3, 7, 10, and 14 to measure percentage of AlamarBlue reduction, which positively correlates to changes in cellular metabolic activity levels, as a measure of cell viability and growth (**Figure 4**). Interestingly, in contrast to previous research, no significant differences were found in cell viability and growth across all timepoints between static and dynamic conditions. This could be attributed to the brief period to which the cardiac patches were subjected to rocking and the lack of fluidic flow changing directions within the

channels of the patch [39]. In addition, cardiac patches cultured in static and rocking conditions exhibited a growth trend which increased throughout most timepoints. On the other hand, although perfused cardiac patches exhibited a growth tendency not significantly different than constructs in static and dynamic conditions at day 3 and day 7, we found significant decrease in cells' metabolic activity after day 7. This decreasing trend in perfused patches could be accredited due to unidirectional flow of HUVEC media causing increased shear stresses on the channel walls, which could reduce the metabolic activity of cells [40]. Nonetheless, further testing must be conducted to conclude the growth trends in static, dynamic, and perfused constructs in a 14-day period and analyze which culture condition is most effective on cellular growth and viability.

Thus far, these results suggest that cardiac patches cultured in static, or dynamic (rocking) conditions would be an optimal group to support cell growth and metabolic activity. Furthermore, for cardiac patches in static and rocking, the significant increase among most timepoints in cellular metabolic activity indicate that, at a prolonged culture period, these cardiac patch systems could effectively sustain HUVEC growth and proliferation. Likewise, the non-significant decrease at day 10 may be indicative of a slower metabolism rather than the complete lack of growth and metabolic activity. In contrast, the decrease in metabolic activity at day 10 and forwards in perfused cardiac patches can be attributed to the limited diffusion of nutrients and oxygen throughout the patch. Given that static and dynamic cardiac constructs presented greatest cellular metabolic activity with a growth trend consistent between both groups, indifferently, the static patches were selected for confocal imaging. In addition, as the greatest cellular metabolic activity was observed at day 7, imaging was performed at this day to qualitatively observe HUVEC organization and morphology.

Characterization of Cellular Organization and Morphology in Vascular Networks of Bioprinted Cardiac Patches

The images acquired from confocal microscopy are a qualitative representation of the proliferation and attachment of HUVECs to the channel walls (**Figure 5**). In static conditions, the channels of the cardiac patches showed effective attachment and proliferation in channels 1, 2, and 4. Particularly, HUVECs are shown to form smooth, uniform, and relatively mature endothelium in the interior of the vascular network. These findings suggest that HUVECs can successfully proliferate and grow within the vascular networks of this cardiac patch system. Significantly, these results can be attributed to the effective oxygen and nutrient diffusion throughout the clinically thick construct offered by the embedded vascular channels and their dimensions comparable to the sizes of arterioles in the body [24]. Additionally, GFP imaging of the microchannels of constructs qualitatively suggest the proliferative action of HUVECs within the walls of the pre-engineered vasculature (**Figure 6**). These results suggest that the CAD model, biomaterials, and culture conditions were adequate to maintain living cells within the channel walls. Moreover, confocal images of the staining of the cell nucleus show the channels have been cellularized as well as the HUVEC attachment and formation of a uniform endothelium throughout the lumen of the vascular channels (**Figure 7**). However, the attachment of HUVECs on the channel walls does not represent a uniform coverage of the lumen of the vasculature, which could be accredited to the low stiffness of the construct that hinders strong binding of cells to the channel surface at the given flow rate. Further optimization of flow rate as well as channel wall stiffness should be conducted in future studies to translate the results into an improved endothelialization of the channel walls.

Overall, in comparison to the formation of endothelium within channels 1, 2, and 4, immunofluorescence imaging qualitatively shows greater proliferation and attachment of HUVECs to the walls in channel 1 but decreases in channel 2 and 4, respectively, which can be ascribed to the smaller diameters of these channels. Further optimizations of the channel 4 diameter should be elaborated on to further understand their impact on cellular survival and metabolic activity. In general, these findings from confocal microscopy suggest the biocompatibility and suitability of gelMA prints to sustain biological cues and mimic the ECM. Furthermore, the results propose the effectiveness of the intrinsic vasculature to allow for oxygen and nutrient diffusion within the microchannels and throughout the 3 mm thickness of the cardiac construct.

In this study, we demonstrate the successful bioprinting of gelMA cardiac constructs with perfusable microchannels. Effectively, *in vitro*, HUVECs seeded throughout a 14-day culture were metabolically active and formed a mature smooth endothelium within the walls of the vascular network, which suggest the cardiac patch design and culture to be effective for HUVEC survival and proliferation. Moving forward, this cardiac patch system with perfusable vascular networks can be applied *in vitro* to create improved 3D models to regenerate cardiac tissue after an irreversible ischemic event and apply them *in vivo* to study their regenerative capacity.

Future Work

For future works, these cardiac patch systems can be 3D bioprinted using gelMA containing iPSCs differentiated into cardiomyocytes and endothelial cells. This would allow us to evaluate the microenvironment of cardiac scaffolds to support cardiomyocyte growth and function, and endothelialization of the vascular networks. Furthermore, future studies can apply the bioprinted

cardiac patches *in vitro* and *in vivo* to study the response of cardiomyocytes to epicardial paracrine peptides, such as the pro-proliferative follistatin-like 1 (FSTL 1) peptide, which has been reported to promote cardiomyocyte proliferation and regeneration of the ischemic myocardium. Ultimately, multiple iterations of the cardiac patch systems fabricated in this work can be developed to investigate the most effective, biocompatible patch devices with functional endothelialized pre-engineered vascular networks, which can repair and regenerate cardiac tissue post-MI.

CHAPTER 6

CONCLUSION

In this study, we investigated the fabrication of a 3D bioprinted cardiac patch device incorporated with perfusable microchannels and evaluated *in vitro* the endothelial cell growth to create fully endothelialized functional vascular networks within the patch. The results from this study suggest that the 3D model of the cardiac patch system with perfusable vasculature can be successfully bioprinted using soft gelMA hydrogel bioinks, while printing the channels with sacrificial pluronic. Furthermore, the cardiac patches designed showed enhanced endothelialization of the embedded channels and high cellular metabolic activity throughout the two-week culture periods. However, further optimization of the perfusion system, channel wall stiffnesses, and culture conditions should be conducted in the future. In addition, future studies can include bioprinting the cardiac patches with iPSCs differentiated into cardiomyocytes and endothelial cells or the incorporation of cardiogenic paracrine factors to promote greater cardiomyocyte proliferation and regeneration of the ischemic myocardium. Overall, this novel platform provides an alternative approach for 3D bioprinting cardiac patch devices with perfusable vascular networks which can be implemented both *in vitro* and *in vivo* to address current challenges in cardiac regeneration and MI therapies.

REFERENCES

[1] J.M. Singelyn, J.A. DeQuach, S.B. Seif-Naraghi, R.B. Littlefield, P.J. Schup-Magoffin, K.L. Christman, Naturally derived myocardial matrix as an injectable scaffold for cardiac tissue engineering, Biomaterials 30(29) (2009) 5409-16.

[2] M.C. Bahit, A. Kochar, B. Granger Christopher, Post-Myocardial Infarction Heart Failure, JACC: Heart Failure 6(3) (2018) 179-186.

[3] D. Rosamond Wayne, E. Chambless Lloyd, G. Heiss, H. Mosley Thomas, J. Coresh, E. Whitsel, L. Wagenknecht, H. Ni, R. Folsom Aaron, Twenty-Two–Year Trends in Incidence of Myocardial Infarction, Coronary Heart Disease Mortality, and Case Fatality in 4 US Communities, 1987–2008, Circulation 125(15) (2012) 1848-1857.

[4] W.Q. Wu, S. Peng, Z.Y. Song, S. Lin, Collagen biomaterial for the treatment of myocardial infarction: an update on cardiac tissue engineering and myocardial regeneration, Drug Deliv Transl Res 9(5) (2019) 920-934.

[5] S. McMahan, A. Taylor, K.M. Copeland, Z. Pan, J. Liao, Y. Hong, Current advances in biodegradable synthetic polymer based cardiac patches, Journal of Biomedical Materials Research Part A 108(4) (2020) 972-983.

[6] S. Anil Kumar, M. Alonzo, S.C. Allen, L. Abelseth, V. Thakur, J. Akimoto, Y. Ito, S.M. Willerth, L. Suggs, M. Chattopadhyay, B. Joddar, A Visible Light-Cross-Linkable, Fibrin-Gelatin-Based Bioprinted Construct with Human Cardiomyocytes and Fibroblasts, ACS Biomater Sci Eng 5(9) (2019) 4551-4563.

[7] H. Cui, C. Liu, T. Esworthy, Y. Huang, Z.-x. Yu, X. Zhou, H. San, S.-j. Lee, S.Y. Hann, M. Boehm, M. Mohiuddin, J.P. Fisher, L.G. Zhang, 4D physiologically adaptable cardiac patch: A 4-month in vivo study for the treatment of myocardial infarction, Science Advances 6(26) (2020) eabb5067.

[8] T. Su, K. Huang, M.A. Daniele, M.T. Hensley, A.T. Young, J. Tang, T.A. Allen, A.C. Vandergriff, P.D. Erb, F.S. Ligler, K. Cheng, Cardiac Stem Cell Patch Integrated with Microengineered Blood Vessels Promotes Cardiomyocyte Proliferation and Neovascularization after Acute Myocardial Infarction, ACS Applied Materials & Interfaces 10(39) (2018) 33088-33096.

[9] A. Schwab, R. Levato, M. D'Este, S. Piluso, D. Eglin, J. Malda, Printability and Shape Fidelity of Bioinks in 3D Bioprinting, Chemical Reviews 120(19) (2020) 11028-11055.

[10] S. Vijayavenkataraman, W.C. Yan, W.F. Lu, C.H. Wang, J.Y.H. Fuh, 3D bioprinting of tissues and organs for regenerative medicine, Adv Drug Deliv Rev 132 (2018) 296-332.
[11] H. Rastin, R.T. Ormsby, G.J. Atkins, D. Losic, 3D Bioprinting of Methylcellulose/Gelatin-Methacryloyl (MC/GelMA) Bioink with High Shape Integrity, ACS Applied Bio Materials 3(3) (2020) 1815-1826.

[12] I. Pepelanova, K. Kruppa, T. Scheper, A. Lavrentieva, Gelatin-Methacryloyl (GelMA) Hydrogels with Defined Degree of Functionalization as a Versatile Toolkit for 3D Cell Culture and Extrusion Bioprinting, Bioengineering 5(3) (2018) 55.

[13] A. Roy, V. Saxena, L.M. Pandey, 3D printing for cardiovascular tissue engineering: a review, Materials Technology 33(6) (2018) 433-442.

[14] D. Richards, J. Jia, M. Yost, R. Markwald, Y. Mei, 3D Bioprinting for Vascularized Tissue Fabrication, Ann Biomed Eng 45(1) (2017) 132-147.

[15] H. Cui, S. Miao, T. Esworthy, X. Zhou, S.-j. Lee, C. Liu, Z.-x. Yu, J.P. Fisher, M. Mohiuddin, L.G. Zhang, 3D bioprinting for cardiovascular regeneration and pharmacology, Advanced Drug Delivery Reviews 132 (2018) 252-269.

[16] D.B. Kolesky, K.A. Homan, M.A. Skylar-Scott, J.A. Lewis, Three-dimensional bioprinting of thick vascularized tissues, Proc Natl Acad Sci U S A 113(12) (2016) 3179-84.

[17] S. Kyle, Z.M. Jessop, A. Al-Sabah, I.S. Whitaker, ‘Printability' of Candidate Biomaterials for Extrusion Based 3D Printing: State-of-the-Art, Advanced Healthcare Materials 6(16) (2017) 1700264.

[18] T.J. Hinton, Q. Jallerat, R.N. Palchesko, J.H. Park, M.S. Grodzicki, H.-J. Shue, M.H. Ramadan, A.R. Hudson, A.W. Feinberg, Three-dimensional printing of complex biological structures by freeform reversible embedding of suspended hydrogels, Science Advances 1(9) (2015) e1500758.

[19] M. Alonzo, S. AnilKumar, B. Roman, N. Tasnim, B. Joddar, 3D Bioprinting of cardiac tissue and cardiac stem cell therapy, Transl Res 211 (2019) 64-83.

[20] D. Bejleri, B.W. Streeter, A.L.Y. Nachlas, M.E. Brown, R. Gaetani, K.L. Christman, M.E. Davis, A Bioprinted Cardiac Patch Composed of Cardiac-Specific Extracellular Matrix and Progenitor Cells for Heart Repair, Advanced healthcare materials 7(23) (2018) e1800672.

[21] M. Alonzo, S.A. Kumar, S. Allen, M. Delgado, F. Alvarez-Primo, L. Suggs, B. Joddar, Hydrogel scaffolds with elasticity-mimicking embryonic substrates promote cardiac cellular network formation, Prog Biomater 9(3) (2020) 125-137.

[22] S. Xiao, T. Zhao, J. Wang, C. Wang, J. Du, L. Ying, J. Lin, C. Zhang, W. Hu, L. Wang, K. Xu, Gelatin Methacrylate (GelMA)-Based Hydrogels for Cell Transplantation: an Effective Strategy for Tissue Engineering, Stem Cell Rev Rep 15(5) (2019) 664-679.

[23] K. Yue, G. Trujillo-de Santiago, M.M. Alvarez, A. Tamayol, N. Annabi, A. Khademhosseini, Synthesis, properties, and biomedical applications of gelatin methacryloyl (GelMA) hydrogels, Elsevier, 2015, pp. 254-271.

[24] M. Radisic, J. Malda, E. Epping, W. Geng, R. Langer, G. Vunjak-Novakovic, Oxygen gradients correlate with cell density and cell viability in engineered cardiac tissue, Biotechnology and Bioengineering 93(2) (2006) 332-343.

[25] Y. Xu, Y. Hu, C. Liu, H. Yao, B. Liu, S. Mi, A Novel Strategy for Creating Tissue-Engineered Biomimetic Blood Vessels Using 3D Bioprinting Technology, Materials (Basel) 11(9) (2018).
[26] D.B. Kolesky, R.L. Truby, A.S. Gladman, T.A. Busbee, K.A. Homan, J.A. Lewis, 3D bioprinting of vascularized, heterogeneous cell-laden tissue constructs, Adv Mater 26(19) (2014) 3124-30.

[27] R. Gaetani, D.A. Feyen, V. Verhage, R. Slaats, E. Messina, K.L. Christman, A. Giacomello, P.A. Doevendans, J.P. Sluijter, Epicardial application of cardiac progenitor cells in a 3D-printed gelatin/hyaluronic acid patch preserves cardiac function after myocardial infarction, Biomaterials 61 (2015) 339-48.

[28] W. Zhu, X. Qu, J. Zhu, X. Ma, S. Patel, J. Liu, P. Wang, C.S.E. Lai, M. Gou, Y. Xu, K. Zhang, S. Chen, Direct 3D bioprinting of prevascularized tissue constructs with complex microarchitecture, Biomaterials 124 (2017) 106-115.

[29] Y.C. Chen, R.Z. Lin, H. Qi, Y. Yang, H. Bae, J.M. Melero-Martin, A. Khademhosseini, Functional Human Vascular Network Generated in Photocrosslinkable Gelatin Methacrylate Hydrogels, Adv Funct Mater 22(10) (2012) 2027-2039.

[30] K. Wei, V. Serpooshan, C. Hurtado, M. Diez-Cuñado, M. Zhao, S. Maruyama, W. Zhu, G. Fajardo, M. Noseda, K. Nakamura, X. Tian, Q. Liu, A. Wang, Y. Matsuura, P. Bushway, W. Cai, A. Savchenko, M. Mahmoudi, M.D. Schneider, M.J. van den Hoff, M.J. Butte, P.C. Yang, K. Walsh, B. Zhou, D. Bernstein, M. Mercola, P. Ruiz-Lozano, Epicardial FSTL1 reconstitution regenerates the adult mammalian heart, Nature 525(7570) (2015) 479-85.

[31] H. Shirahama, B.H. Lee, L.P. Tan, N.-J. Cho, Precise Tuning of Facile One-Pot Gelatin Methacryloyl (GelMA) Synthesis, Sci Rep 6(1) (2016) 31036.

[32] H. Cui, S. Miao, T. Esworthy, X. Zhou, S.J. Lee, C. Liu, Z.X. Yu, J.P. Fisher, M. Mohiuddin, L.G. Zhang, 3D bioprinting for cardiovascular regeneration and pharmacology, Adv Drug Deliv Rev 132 (2018) 252-269.

[33] J. Yin, M. Yan, Y. Wang, J. Fu, H. Suo, 3D Bioprinting of Low-Concentration Cell-Laden Gelatin Methacrylate (GelMA) Bioinks with a Two-Step Cross-linking Strategy, ACS Applied Materials & Interfaces 10(8) (2018) 6849-6857.

[34] A.C. Daly, P. Pitacco, J. Nulty, G.M. Cunniffe, D.J. Kelly, 3D printed microchannel networks to direct vascularisation during endochondral bone repair, Biomaterials 162 (2018) 34-46.

[35] M. Shokouhimehr, A.S. Theus, A. Kamalakar, L. Ning, C. Cao, M.L. Tomov, J.M. Kaiser, S. Goudy, N.J. Willett, H.W. Jang, C.N. LaRock, P. Hanna, A. Lechtig, M. Yousef, J.D.S. Martins, A. Nazarian, M.B. Harris, M. Mahmoudi, V. Serpooshan, 3D Bioprinted Bacteriostatic Hyperelastic Bone Scaffold for Damage-Specific Bone Regeneration, Polymers 13(7) (2021) 1099.

[36] A.D. Cetnar, M.L. Tomov, L. Ning, B. Jing, A.S. Theus, A. Kumar, A.N. Wijntjes, S.R. Bhamidipati, K.P. Do, A. Mantalaris, J.N. Oshinski, R. Avazmohammadi, B.D. Lindsey, H.D. Bauser-Heaton, V. Serpooshan, Patient-Specific 3D Bioprinted Models of Developing Human Heart, Advanced Healthcare Materials n/a(n/a) 2001169.

[37] A.A. Aldana, F. Valente, R. Dilley, B. Doyle, Development of 3D bioprinted GelMA-alginate hydrogels with tunable mechanical properties, Bioprinting 21 (2021) e00105.

[38] G. Ying, N. Jiang, C. Yu, Y. Zhang, Three-dimensional bioprinting of gelatin methacryloyl (GelMA), Bio-Design and Manufacturing 1 (2018) 215-224.

[39] M.B. Esch, J.-M. Prot, Y.I. Wang, P. Miller, J.R. Llamas-Vidales, B.A. Naughton, D.R. Applegate, M.L. Shuler, Multi-cellular 3D human primary liver cell culture elevates metabolic activity under fluidic flow, Lab on a Chip 15(10) (2015) 2269-2277.

[40] S. Ting, A. Chen, S. Reuveny, S. Oh, An intermittent rocking platform for integrated expansion and differentiation of human pluripotent stem cells to cardiomyocytes in suspended microcarrier cultures, Stem Cell Research 13(2) (2014) 202-213.